OCVD Measurement of Ambipolar and Minority Carrier Lifetime in 4H-SiC Devices: Relevance of the Measurement Setup

OCVD measurement of ambipolar and minority carrier lifetime in 4H-SiC devices: relevance of the measurement set-up

Giovanna Sozzi, *Member, IEEE*, Sergio Sapienza,
Roberta Nipoti, *Member, IEEE*, and Giovanni Chiorboli

***Abstract*—The Open Circuit Voltage Decay (OCVD) method is a well-known technique for performing electrical measurements of carrier lifetime: the main advantages lie in the simple setup and the possibility of performing measurements in commercial devices without the need of removing the package, as for optical methods. Despite several researchers have reported carrier lifetimes measured by the OCVD method in different devices, there has been little discussion about the potential effect of experimental set-up on the obtained results. By comparing the outputs of experimental measurements with those of numerical simulations, this study investigates the overlooked effect of the OCVD measurement set-up on the former. Due to the growing importance of SiC-based devices, the analysis is applied to a 4H-SiC PiN diode. Two main points are addressed: i) the effect of circuit set-up on the ambipolar lifetime is discussed and a method, originally developed for improving the estimate of low-level carrier lifetime in OCVD measurements, is used to correct the measured lifetime for this influence; ii) the origin of the local minimum eventually appearing in the lifetime versus time curves is also investigated. It is found that the minimum can also be related to the time constant of the experimental set-up, arising doubts about the usual interpretation of this minimum as the minority carrier lifetime. A method is thus proposed to help discriminate between the two interpretations.**

***Index Terms*— Carrier lifetime, OCVD, PiN diodes, 4H-SiC.**

I. Introduction

Silicon Carbide power device have been gaining an increasingly important role in a variety of power systems, such as photovoltaic converters, power supplies, motor control, electric/hybrid vehicles or telecommunications, that can benefit from the excellent physical properties of SiC [1].

Among the different SiC polytypes, presently, 4H-SiC has the larger wafer diameter and the better electronic quality. Commercial SiC power devices are made of the 4H-SiC polytype.

Depending on the specific device and application, the major features of SiC power devices include low on-resistance and fast switching performance typical of MOSFETs, SBD or JBD, but also potential drawbacks as in the case of the switching loss associated with the MOSFETs' body diode.

Bipolar devices are limited in their switching-speed by the stored minority carrier that also determines the large reverse recovery during turn-off, that however is lower than in their Silicon counterparts.

As known, the carrier lifetime is the key parameter for a reliable prevision of device features like the on-resistance and the switching frequency, that control the forward voltage drop and the reverse recovery time, respectively.

Due to the growing importance of SiC-based electronic devices, an accurate estimate of carrier lifetime and its dependence on temperature is thus a fundamental step towards the development of models to be used at the early design stage of a device or to evaluate the performance of a power converter, or, for example, the behavior of a MOSFET's body diode.

Although several reports on the SiC physical properties are available, the accuracy and investigated temperature range need further investigations: for that reason, we performed OCVD measurements on an unpackaged 4H-SiC PiN diode that was internally manufactured. The fact that the structure, doping, and processing data of such diode are known allows us to verify the experimental findings through numerical analysis of the diode behavior.

As known, the carrier lifetime can be measured either by optical (such as the time-resolved photoluminescence, TRPL, the photo-conductance decay, PCD, or the time-resolved free carrier absorption method, FCA)[2] and electrical methods (such as the current recovery time (CRT)[3] and the open-circuit voltage decay (OCVD) [4]). In general, optical measurements can be affected by surface recombination, while the electrical ones are mainly influenced by the experimental method used [5].

Regarding the electrical methods, the CRT technique investigates the drift region next to the pn junction, where damage induced by ion-implantation may be present and strongly reduces the minority carrier lifetime, in the case of ion-implanted emitter [6]. On the other hand, the OCVD technique results in a mean carrier lifetime averaged over the drift region.

Moreover, the carrier lifetime measured by electrical methods often deals with the difficulty of a reliable quotation of the lifetime that may depend on the current-injection and the device geometry, as shown in [7].

The purpose of this paper is to investigate the influence of the experimental set-up on OCVD measurement of both ambipolar (or high-level) and minority carrier lifetime of PiN

[M]anuscript received March 29, 2021.
G. Sozzi, S. Sapienza, and G. Chiorboli are with the Department of Engineering and Architecture, Università di Parma, I-43124 Parma, Italy (e-mail: giovanna.sozzi@unipr.it).
R. Nipoti is with the CNR-IMM of Bologna, I-40129 Bologna, Italy.

diodes that must be carefully analyzed, as we will show.

The relevance of R-C effects, attributable to both measurement set-up and device junction capacitance and leakage, has recently attracted scientific attention for the solar cells [8–10], while was not sufficiently considered for SiC diodes in high-injection conditions.

We also discuss the origin of the local minimum appearing in the measured lifetime versus time curve after biasing the diode in high-injection regime, commonly interpreted as the minority carrier lifetime, that we show may be related to the circuit time constant.

Results can be also useful during the characterization of the body diode of a MOSFET as we recently showed [11], or the drift region of IGBT or BJT.

II. Device and Methods

A. Measured Device

The measured PiN diode belongs to a family of vertical diodes fabricated by ion implantation on commercial n-type 8° off-axis <0001> 4H-SiC homo-epitaxial wafer. The bulk wafer thickness is 372 μm and its resistivity is 0.021 Ω·cm. The epi-layer is 25 μm thick and has a net donor concentration of 3×10^{15} cm^{-3}. The p^+ emitters are circular of 150-1000 μm diameters obtained by selected area Al^+ ion hot implantation with $2\cdot10^{20}$ cm^{-3} dopant concentration over a depth of about 200 nm from the wafer surface. Annealing temperature and time are 1950°C and 5 min, respectively. No surface passivation is performed.

Anode and cathode ohmic contacts are e-gun evaporated Ti/Al (80 nm/350 nm) and Ni (150 nm), respectively. After alloying, anode contacts are made thicker by sputtered 350 nm Al (2% Si). Anode contacts are circular and centered on the anode region but with a 50 μm-smaller diameter. More details on diode fabrication are in [12]. Diodes of 150 μm diameter have been used for this study.

The diode ambipolar carrier lifetime is measured in air at room temperature (RT) with the OCVD method [4]. In this technique the diode is driven in the forward conduction region by a bias current which is suddenly terminated: the consequent voltage decay, $V_{out}(t)$, which is sustained by the carriers injected into the base of the diode, is recorded.

The carrier lifetime is extracted from the slope value dV_{out}/dt of the linear trait appearing after the voltage drop (this latter ideally due only to the diode series resistance [13] by (1)):

$$\tau = -\,n\,\frac{kT}{q}\cdot\left(\frac{dV_{out}}{dt}\right)^{-1} \qquad (1)$$

with k, T, and q, Boltzmann constant, absolute temperature, and elementary electron charge, respectively, and where the factor *n* is 1 or 2 depending on whether the injection level is low or high [14]. For n =2 (1), the high-level (low-level) lifetime τ_{HL} (τ_{LL}) is obtained.

B. Experimental set-up

The block diagram of the experimental set-up used for implementing the OCVD measurements is shown in Fig.1. The SMU (Source-Monitor Unit) Keithley 2400 provides a bias forward current density, J_B, of 210 A/cm^2. A mercury wetted relay from Pickering with a maximum operating current of 3 A and an open circuit resistance > 10^{12} Ω, is used to separate the diode polarization unit from the device to avoid the bounce effects during switching, as suggested in [15]. The relay opening is controlled by a Philips PM5781 programmable pulse generator. The relay turn-on time is of the order of 10 ns. $V_{out}(t)$ is acquired with Tektronix P6139A passive probes connected to the eight-bit Tektronix DPO7254 Digital oscilloscope with a sampling rate up to 20 GSa/s (additional details on the experimental set-up can be found in [7]).

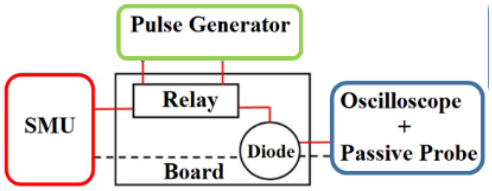

Fig. 1. Experimental set-up used for OCVD measurements: block diagram of the test bench - the central square block is the PCB. The Source-Monitor Unit (SMU) provides the forward current to bias the diode.

C. OCVD measurements

In the initial trait of the V_{out} transient after the voltage drop, the charge stored in the drift region is large, and the dominant capacitance contribution is the diffusive one. This charge returns to the equilibrium value through recombination processes and the V_{out} vs time curve approaches a linear decay [16], as qualitatively illustrated in Fig. 2 ("ideal decay" curve), with the slope equal to $dV_{out}/dt=-nkT/q\cdot1/\tau$.

As the decay proceeds, the diffusion charge exponentially reduces with time and the junction capacitance, Cj, increases. When the junction capacitance is appreciable, the voltage decay starts deviating from the ideal-case and slows-down ("junction capacitance" curve in Fig. 2); also external capacitances, as the one due to the measurements set-up, can add to the Cj enhancing the effect.

Similarly, in the presence of a resistance in parallel to the diode, the voltage decay can deviate from the ideal-case since carriers may leave the diode neutral regions through the resistive parallel path; in this case the decay accelerates in comparison to the ideal case and the measured lifetime is underestimated ("shunt resistance" curve in Fig. 2).

As suggested by Green [17], by observing the differential of the voltage decay it is possible to cancel out the effect of both junction capacitance and shunt resistance that determine the departure from the ideal linear relationship of lifetime on voltage (as described by (1)) by connecting extra resistance or capacitance in parallel with the diode: the compensated voltage

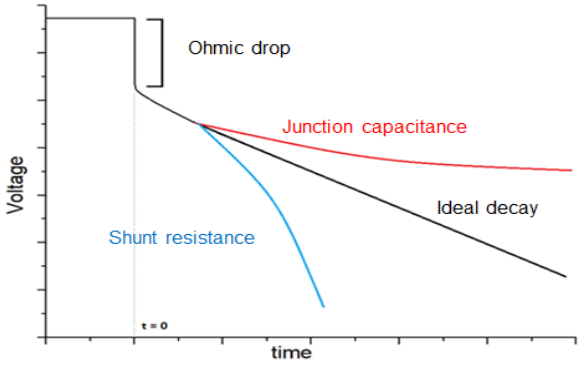

Fig. 2 Typical trends of open circuit voltage decays showing the ideal decay curve and the effect of junction capacitance, and shunt resistance.

decay will result in a constant dV_{out}/dt, as in the ideal case, over a larger time interval, facilitating the extraction of the carrier lifetime from the measured curve.

The measured diode has shown a capacitance-dominated behavior, so that an extra-resistance, R_{EXT}, has been connected in parallel to the diode, as explained in the following.

D. Diode model and numerical simulation

A three-dimensional numerical model of the measured diode has been realized with the Sentaurus-tcad suite.

The cylindrical symmetry of the diode, allows to simulate half of the cross-section on a symmetry plane, i.e., the section inside the black frame in Fig. 3a, while the 3D current is calculated in a post-simulation step. In particular, the anode region is circular with a diameter of 150 µm; the metal contact is centered on it but with a 50 µm-smaller diameter.

The diode behavior is described by the Poisson, electron and hole continuity, and drift-diffusion equations. Specific models for 4H-SiC account for band-gap narrowing [18] and incomplete ionization of dopants [19]. The carrier lifetime is assumed to be controlled only by traps related to the carbon vacancies [20, 21] systematically found in 4H-SiC n-doped epi-layers [12, 22]. Recombination processes are described by the Shockley-Read-Hall statistic.

The fundamental parameters of 4H-SiC and additional details about the diode simulation can be found in our previous works [23].

The OCVD measurement is simulated by introducing the 3D diode model into the mixed-mode circuit of Fig. 3b, where the remaining components, due to the experimental set-up, are described by spice-like compact models. In particular, R_{scope} = 10 MΩ and C_{scope} = 8 pF are the scope resistance capacitances, respectively, R_{EXT} is the variable external resistor used in measurements, and C_{TOT} is the parallel of circuit parasitic ≈ 1 pF plus the relay and scope capacitance (5 + 8 pF).

In the OCVD simulations of the diode, the device is firstly biased in forward condition by the same current density, J_{BIAS}, of measurements, afterward the switch is opened and the open circuit voltage decay evaluated; the simulations are repeated for the same R_{EXT} values used in measurements and for additional values of 10 and 100 kΩ.

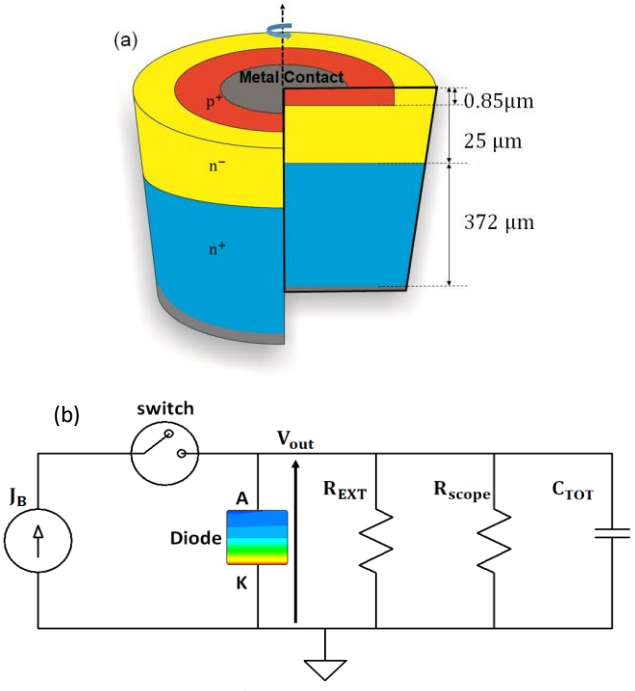

Fig. 3. a) Schematic drawing of the diode model; b) mixed-mode circuit used in the numerical simulation of diode OCVD. The diode model and circuit parameters are described in the text.

III. RESULTS AND DISCUSSIONS

A. Measured OCVD curves and ambipolar carrier lifetime

The measured open-circuit voltage decay curves of a 150 µm-diameter diode are shown in Fig. 4 for R_{EXT} values varying from 270 kΩ to 10 MΩ; the forward bias current density, J_{BIAS}, of about 210 A/cm^2 is switched off at time 0 µs.

The voltage step appearing at the relay opening is due to the diode internal series resistance, as explained in [13]. After the current is suddenly terminated, a potential remains across the junctions due to the presence of excess carriers in the drift region: this potential decays in time as the excess carriers return to equilibrium.

The OCVD curves of Fig.4 are initially filtered according to [24] to remove noise, then the carrier lifetime is calculated from the slope value dV_{out}/dt of the linear trait after the voltage drop [14], as explained in section IIA (Fig.5).

The behavior of lifetime appearing in Fig.5a for 250 ns after the voltage drop is not significant as it is the result of the numerical filtering algorithm.

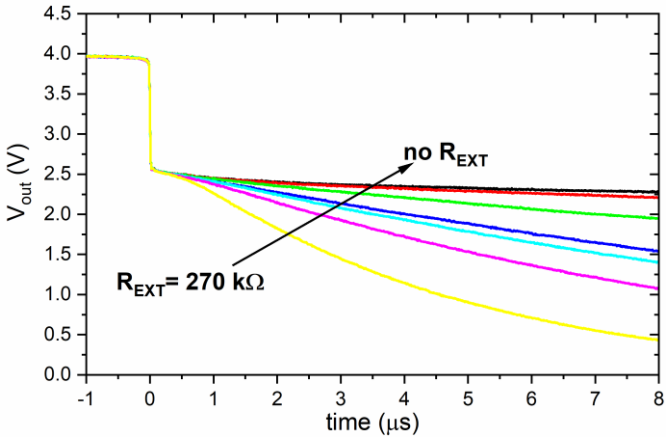

Fig. 4. Measured open circuit voltage decays for a bias current density J_{BIAS} = 210A/cm^2 and variable external resistance, R_{EXT}.

The parasitic inductance of the device and measuring circuit can affect the voltage decay immediately after the relay opening and might add some ringing to the voltage decay, making more complicated the estimation of the reciprocal slope.

In the presence of ringing, since the OCVD technique requires a sudden open circuit condition [5], a reasonable approach could be to decrease the bias current, which however must remain high enough to ensure the high-injection condition required in the case of τ_{HL} estimation.

The ambipolar carrier lifetime, τ_{HL}, calculate for each $V_{out}(t)$ curve in Fig. 4 is reported in Table I for different R_{EXT}.

TABLE I

EXTRACTED τ_{MIN} (CALCULATED @ V_{OUT}=2.2 V) AND τ_{HL} FOR EACH VALUE OF SHUNT RESISTANCE, R_{EXT}, AND CIRCUIT EQUIVALENT RESISTANCE, $R_{||}$.

R_{EXT} (MΩ)	τ_{HL} (ns)	$R_{||}$ (MΩ)	τ_{MIN} (ns)
0.27	175	0.263	116
0.56	296	0.53	221
0.82	360	0.758	307
1	380	0.91	372
2.2	≈ 510	1.8	-
10	≈ 630	5	-
∞ (no R_{EXT})	≈ 680	10	-

The extracted τ_{HL} shows a strong dependence on the R_{EXT} values, spanning from 175 ns to ≈ 680 ns as R_{EXT} increases from 270 kΩ to infinity (in this last case only the resistor R_{scope} = 10 MΩ is connected in parallel to the diode).

How to identify the reliable τ_{HL} among the values of Table I is shown hereinafter.

Fig. 5a plots the computed $\tau = -(2kT/q)\cdot(dV_{out}/dt)^{-1}$ versus time for each curve of Fig. 4. Two regions can be identified: region I where curves show a local maximum or an inflection point, and region II where the curves show a local minimum.

τ_{HL} should thus be estimated from the local maximum visible in region I for R_{EXT} in the interval 270 kΩ (yellow curve) to 2.2 MΩ (green curve), while for larger R_{EXT} the capacitive effect is dominant and the local maximum is replaced by an inflection point, as in the cases of R_{EXT} = 10 MΩ (red curve) and $R_{EXT} = \infty$ (i.e., no R_{EXT}, black curve) shown in Fig. 5a.

However, this notable point varies with R_{EXT} as reported in Table I. As a consequence, the choice of the τ value that should be assigned to τ_{HL} becomes questionable; that is, depending on the equivalent resistance and capacitance of the measurement circuit, the lifetime values extracted with the OCVD technique can be quite different.

One possible implication of the observed behavior is that a single measurement of the diode voltage decay cannot rule out the influence of the experimental set-up on the measurement, being it a simple scope or a complex electronic circuit as in [15].

Fig. 5b plots the differential of the voltage decay $|dV_{out}/dt|$ versus decay time as suggested in [17] for each curve of Fig. 5a. For R_{EXT} < 1 MΩ, the curves of Fig. 5b show the typical shape of a shunt resistance-dominated decay, while for R_{EXT} > 10 MΩ, they appear to be controlled by the diode junction capacitance, Cj, in parallel with C_{TOT}.

The $|dV_{out}/dt|$ curve discriminating between the shunt resistance- and the capacitance-dominated regime is

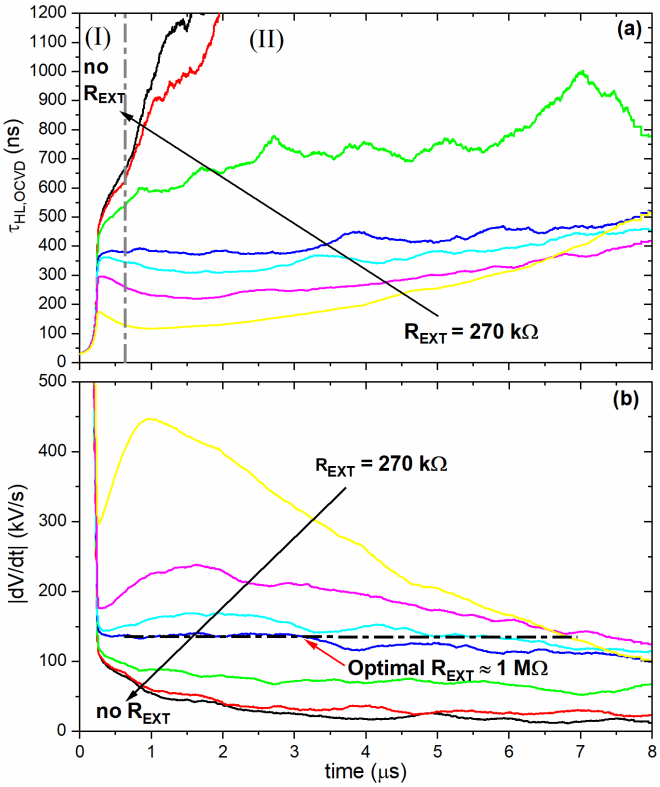

Fig. 5. a) Measured lifetime calculated as $\tau = (2kT/q)\,(dV_{out}/dt)^{-1}$ versus time. The vertical dotted-dashed marks the regions of local maxima and inflection points (reg. I) and minima (reg. II); b) Differential of the open circuit voltage decay versus time for a bias current density J_{BIAS} = 210 A/cm² and different shunt resistance, R_{EXT}.

qualitatively indicated by the dotted-dashed line sketched in Fig. 5b, which represents the ideal diode decay. The corresponding experimental curve superimposes the dotted-dashed line for an optimal shunt resistance of 1 MΩ, as shown by the blue curve in Fig. 5b: it corresponds to a lifetime of 380 ns (see the blue curve in Fig. 5a).

A reliable determination of the carrier lifetime thus requires readjusting the R_{EXT} value to move $|dV_{out}/dt|$ towards the ideal voltage decay, i.e. the compensated curve.

B. Minority carrier lifetime

Previous studies [15, 24] have reported that the OCVD waveform of a diode initially biased in high-level injection regime exhibits two distinct linear traits, corresponding to a local maximum and a local minimum in the lifetime calculated by (1), respectively related to the ambipolar and minority carrier lifetimes.

In our measurements, we also see a local minimum, but it varies with R_{EXT} (see Fig. 5a, curves from blue to yellow, and also data reported in Table I), raising some doubts about its interpretation as the minority carrier lifetime.

To investigate further the origin of this minimum and the observed dependence on R_{EXT}, we developed the numerical model of the measured diode described in section II, and simulated the open circuit voltage decays.

1) Simulated OCVD curves: minority carrier lifetime estimate

The diode open circuit voltage decay has been simulated both

in the ideal case, i.e., with neither external resistor nor capacitor connected in parallel to the modeled device, and with the same C_{TOT}, R_{scope}, and R_{EXT} used in measurements (R_{EXT} = 10, 100 kΩ are also simulated); in both cases, the diode has been biased with the same J_{BIAS} used in measurements. The diode model and the schematic of the simulated mixed-mode circuit is sketched in Fig. 3b.

Two different combinations of electron, τ_e, and hole, τ_h, lifetimes have been considered in the simulations: i) τ_e = 280 ns and τ_h = 100 ns and ii) $\tau_e = \tau_h$ = 190 ns, both corresponding to the measured high-level lifetime $\tau_{HL} = \tau_e + \tau_h$ = 380 ns.

i) The simulated OCVDs for τ_e = 280 ns and τ_h = 100 ns are shown in Fig. 6 for R_{EXT} ranging from 10 kΩ to ∞ (no R_{EXT}).

In this case, the lifetime extracted from the simulated OCVD curves with (1) shows a local maximum corresponding to the high-level lifetime, τ_{HL}, and a local minimum, τ_{MIN} (Fig. 7a that should be related with the minority carrier lifetime, as in [15, 24]. In particular, since the low level lifetime is obtained by (1) with n = 1, τ_{MIN} should correspond to two-times the low-level lifetime, $\tau_{LL} \approx \tau_h$.

The ideal voltage decay of the diode, i.e. no external resistor or capacitor due to the experimental set-up connected in parallel to the modeled device, is reported as comparison (the black dotted-dashed curve in Fig. 7a): a value of τ_{HL} = 296 ns and τ_{MIN} = 212 ns can be obtained from the compensated curve, the fuchsia one. These values have to be compared with $\tau_e + \tau_h$ = 380 and $2\cdot\tau_h$ = 200 ns defined in the simulations.

τ_{HL} is lower than $\tau_e+\tau_h$ because of the carrier flow from the epi-layer to the heavily doped regions of the device [16], while the slight overestimation of the minority carrier lifetime (106 ns instead of 100 ns) could be further reduced by adjusting the R_{EXT} value (in fact, the same R_{EXT} of measurements are used in simulations).

When the capacitor and resistor of the external circuit with C_{TOT}=14 pF and a R_{EXT}=10 MΩ (red curve in Fig. 7a) are connected in parallel to the diode model, the simulated local minimum slightly increases in value compared to the ideal decay curve due to the effect of the external capacitance, (compare the red and black dotted-dashed lines in Fig. 7a). Moreover, τ_{MIN} is observed to depend on R_{EXT}.

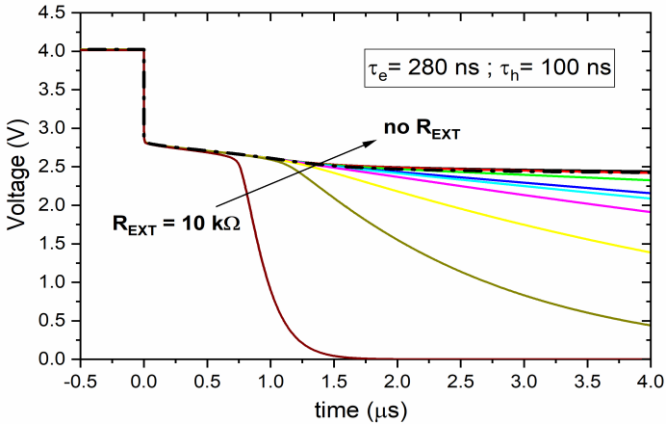

Fig. 6. Simulated open circuit voltage decays for a bias current density J_B = 210 A/cm^2 and variable shunt resistances, R_{EXT}. The black dotted-dashed line corresponds to the ideal diode open-circuit voltage decay.

With R_{EXT} in the range 560 kΩ -10 MΩ (i.e. from fuchsia to red curves in Fig.7a), τ_{MIN} varies between -7% and +6% around the ideal case value, τ_{MIN} = 225 ns.

For R_{EXT} < 560 kΩ, instead, a marked dependence of τ_{MIN} on R_{EXT} appears, with τ_{MIN} suddenly dropping to values that are uncorrelated with the carrier minority lifetime (yellow, dark-green and brown curves).

ii) In the case of equal electron and holes lifetimes $\tau_{HL} = \tau_e + \tau_h$ and $\tau_{MIN} = 2\tau_h$ have the same value so that the local minimum is not visible in the τ_{HL} curves for $R_{EXT} \geq 1$ MΩ (blue line in Fig. 7b).

However, as in the previous case, a local minimum appears as R_{EXT} reduces, largely varying with R_{EXT}, and whose value is uncorrelated with the minority carrier lifetime. The observed strong dependence of τ_{MIN} on R_{EXT}, suggests an influence of the external circuit set-up on the OCVD waveform.

Supposing an exponential decay due to circuit set-up, the slope of the plot of τ_{MIN} versus $R_{||}$ is proportional to the total circuit capacitance C_{TOT}+Cj. In fact, if $|dV_{out}/dt| = V_{out}/(R_{||}\cdot(C_{TOT}+Cj))$, equation (1) with n = 2 modifies to (2):

$$\frac{\tau}{2}\frac{Vout}{v_{th}} = R_{||}\cdot(C_{TOT} + C_j) \qquad (2)$$

where v_{th} is the thermal voltage and $R_{||}$ the circuit equivalent resistance.

The plot of (2) versus $R_{||}$, calculated from the simulated τ_{MIN} in Fig. 7a for 10 kΩ ≤ R_{EXT} ≤270 KΩ (black squares) and

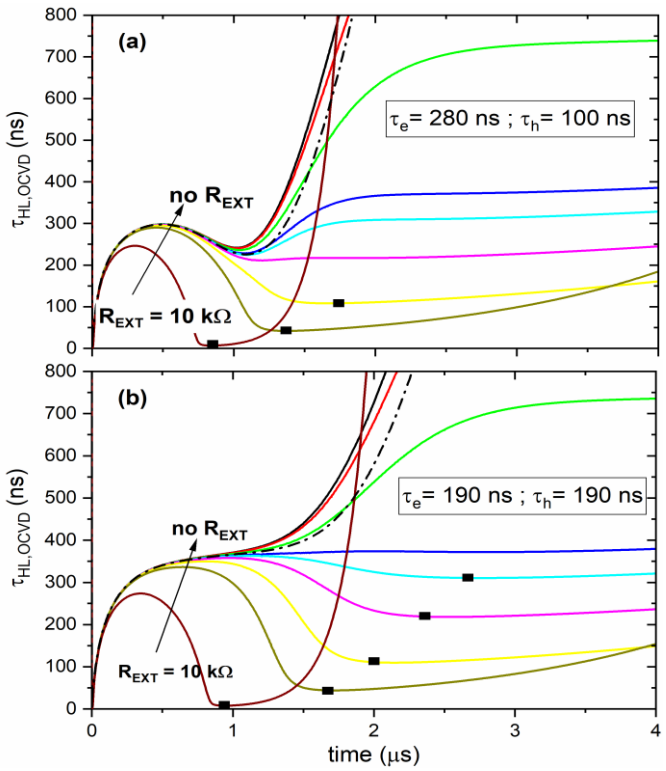

Fig. 7. Lifetime, calculated from the simulated OCVD decays as $\tau = (2kT/q)(dV_{out}/dt)^{-1}$, versus time; electron, τ_e, and hole, τ_h, carrier lifetimes are: a) τ_e = 380 ns, τ_h = 100 ns; b) $\tau_e = \tau_h$ = 190 ns.

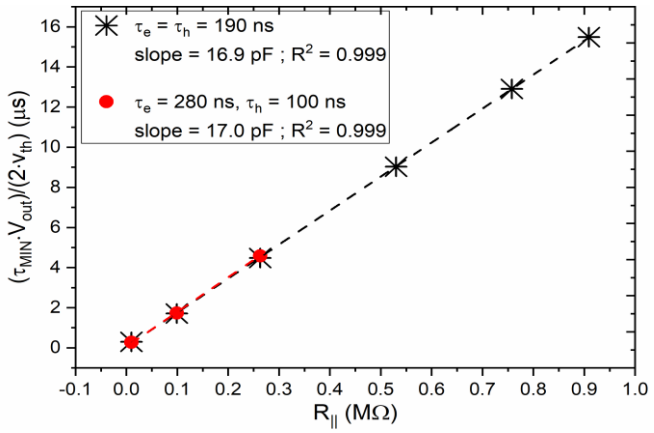

Fig. 8. (τ_{MIN}·Vout)/(2·v_{th}) versus the circuit equivalent resistance $R_{||}$ calculated from the simulated curves of Figs. 7. The dashed lines are the regression lines and R^2 the corresponding correlation coefficient.

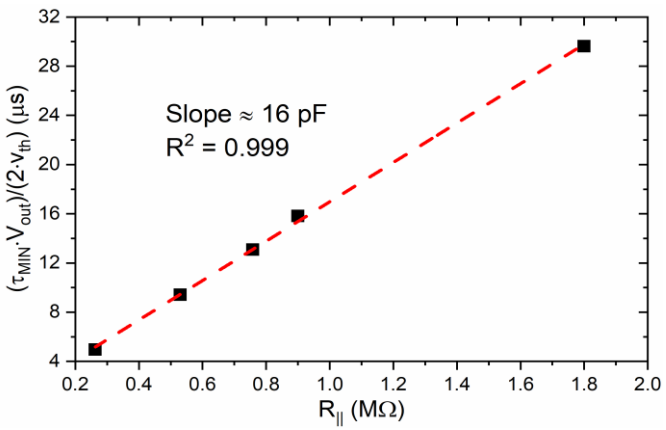

Fig. 10. Measured (τ_{MIN}·Vout)/(2·v_{th}) (full squares) calculated at V_{out}=2.2 V versus the circuit equivalent resistance $R_{||}$. The red dash line is the regression line and R^2 the corresponding correlation coefficient.

Fig. 7b 10 kΩ ≤ R_{EXT} ≤ 820 kΩ (black squares) in the case of an unbalanced and balanced lifetime, respectively, have a slope of about 17 pF as shown in Fig. 8, which is consistent with the sum of 14 pF due to the measurement set-up and about 3 pF of the internal diode capacitance: the interpretation of this quantity as the time constant of the RC circuit is thus demonstrated.

2) Measured OCVD curves: minority carrier lifetime estimate

As anticipated, the measured lifetime curves versus time in region (II) of Fig. 5a, exhibit local minima varying with R_{EXT}: the τ_{MIN} extracted for each R_{EXT} are reported in Table I, and roughly correspond to a V_{out} of about 2.2 V.

These minima have been analyzed in light of the simulation results.

At first, the equivalent resistance of the circuit $R_{||}$ has been calculated as the parallel of R_{EXT}, R_{scope}, and R_d (this latter, extracted from the diode I-V curves at V_{out} = 2.2 V, is larger than 70 MΩ); the resulting $R_{||}$ are reported in Table I.

Secondly, the junction capacitance has been evaluated by C-V measurements made at high frequency (f_0 = 1 MHz) to make the contribution of diffusion capacitance negligible, as explained in [25]: a value of Cj ≈ 2.7 pF is measured for V_{out} = 2.2 V, as depicted in Fig. 9.

Finally, the measured (τ_{MIN}·V_{out})/(2·v_{th}) has been drawn versus $R_{||}$: as shown in Fig. 10, the measured data (symbols) are well interpolated by a straight line whose slope is ≈ 16 pF, to be compared to the sum of Cj ≈ 2.7 pF and C_{TOT} ≈ 14 pF.

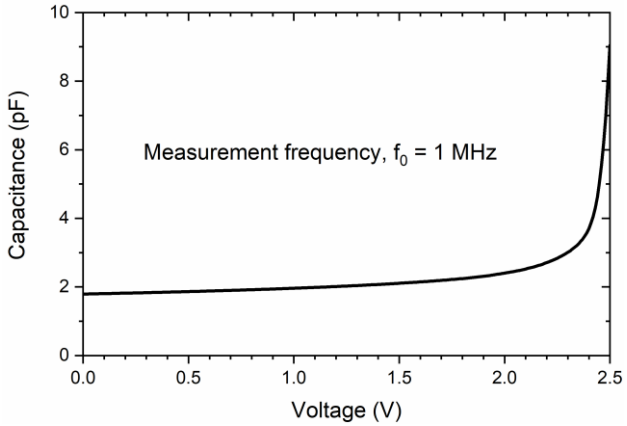

Fig.9. Diode capacitance versus voltage measured at 1 MHz.

This supports the interpretation of τ_{MIN} as determined by the RC constant of the circuit as an alternative to the minority carrier lifetime.

In conclusion, the evidence from this study suggests that the ambipolar and minority carrier lifetimes can be affected by the capacitive (or resistive) behavior of the DUT plus the circuit set-up, causing the departure of the OCVD curve from linearity, so that corrective actions need to be implemented.

The compensation of the capacitive (resistive) behavior of OCVD curves by connecting a resistor (capacitor) in parallel with the DUT, as originally proposed by Green for the minority lifetime measurement, can be used to estimate the ambipolar lifetime cleaned up from the set-up influence.

On the basis of the findings above, we can draw the following indication for a reliable estimate of the ambipolar and minority carrier lifetimes.

a) A first measure of the DUT in the circuit set-up allows discriminating, between an open circuit voltage decay dominated by the capacitance or the shunt resistance.

b) An external resistor, R_{EXT} (as in the present work) or capacitor, has to be connected in parallel to the device to compensate for it, and measurements have to be repeated for different values of R_{EXT} (C_{EXT}).

c) The differential of the OCVD curves for various R_{EXT} (C_{EXT}) allows to identify the optimal R_{EXT} (C_{EXT}), i.e. the one giving a flat curve, from which the ambipolar lifetime can be calculated.

d) In the case, a second linear trait, potentially related to the minority carrier lifetime, appears in measurements, a plot of $\frac{\tau}{2}\frac{Vout}{v_{th}}$ versus the circuit equivalent total resistance, $R_{||}$, can help discriminate between the minority carrier lifetime or the circuit RC time constant.

e) If the experimental points of $\frac{\tau}{2}\frac{Vout}{v_{th}}$ versus $R_{||}$ lie on a straight line, the slope gives the equivalent circuit capacitance, that can be also separately estimated; in this case the local minimum, τ_{MIN}, calculated by (1) is uncorrelated with the minority carrier lifetime.

f) In case point e) does not occur, the minority carrier lifetime can be calculated from the τ_{MIN} of the compensated curve, i.e., the one with the optimal R_{EXT} (or C_{EXT}).

IV. Conclusions

The carrier lifetime measurements by OCVD technique of a 4H-SiC PiN diode has been proven to be heavily affected by the set-up parasitic and scope resistances and capacitances that may cause the departure of the OCVD curve from linearity so that corrective actions and careful analysis of experimental voltage decay curves need to be performed to obtain a reliable estimate of the carrier lifetime.

The method previously proposed by Green to improve the OCVD measurement of minority carrier lifetime, has been shown to be a viable approach to follow for the estimate of the ambipolar carrier lifetime, too.

Moreover, the still considerable ambiguity about the interpretation of the local minimum eventually appearing in the lifetime waveform extracted from the OCVD measurements of a diode initially biased in high-injection regime has been also addressed with the help of numerical simulations. As a result, a method has been proposed to help to clarify the origin of this minimum, commonly attributed to the minority carrier lifetime, that can be also related to the RC constant of the circuit, as demonstrated in the present study.

References

[1] T. Kimoto, "Ultrahigh-voltage SiC devices for future power infrastructure," Eur. Solid-State Device Res. Conf., no. 21226008, pp. 22–29, 2013.

[2] D. K. Schroder and L. G. Rubin, Semiconductor Material and Device Characterization. 2006.

[3] B. Lax and S. F. Neustadter, "Transient response of a p-n junction," J. Appl. Phys., vol. 25, no. 9, pp. 1148–1154, 1954.

[4] S. R. Lederhandler and L. J. Giacoletto, "Measurement of Minority Carrier Lifetime and Surface Effects in Junction Devices," Proc. IRE, vol. 43, no. 4, pp. 477–483, 1955.

[5] M. Derdouri, P. Le, and A. Munoz-Yague, "A comparative study of methods of measuring carrier lifetime in p-i-n devices," IEEE Trans. Electron Devices, vol. 27, no. 11, pp. 2097–2101, Nov. 1980.

[6] M. E. Levinshtein et al., "'Paradoxes' of carrier lifetime measurements in high-voltage SiC diodes," IEEE Trans. Electron Devices, vol. 48, no. 8, pp. 1703–1710, 2001.

[7] G. Sozzi, M. Puzzanghera, G. Chiorboli, and R. Nipoti, "OCVD Lifetime Measurements on 4H-SiC Bipolar Planar Diodes: Dependences on Carrier Injection and Diode Area," IEEE Trans. Electron Devices, no. 1, pp. 1–7, 2017.

[8] O. J. Sandberg, K. Tvingstedt, P. Meredith, and A. Armin, "Theoretical Perspective on Transient Photovoltage and Charge Extraction Techniques," J. Phys. Chem. C, vol. 123, no. 23, pp. 14261–14271, 2019.

[9] K. Tvingstedt et al., "Removing Leakage and Surface Recombination in Planar Perovskite Solar Cells," ACS Energy Lett., vol. 2, no. 2, pp. 424–430, 2017.

[10] D. Kiermasch, A. Baumann, M. Fischer, V. Dyakonov, and K. Tvingstedt, "Revisiting lifetimes from transient electrical characterization of thin film solar cells; A capacitive concern evaluated for silicon, organic and perovskite devices," Energy Environ. Sci., vol. 11, no. 3, pp. 629–640, 2018.

[11] S. Sapienza et al., "Correlation between OCVD carrier lifetime vs temperature measurements and reverse recovery behavior of the body diode of SiC power MOSFETs," Microelectron. Reliab., vol. 113, no. September, p. 113937, 2020.

[12] R. Nipoti, M. Puzzanghera, G. Sozzi, and R. Menozzi, "Perimeter and Area Components in the I-V Curves of 4H-SiC Vertical p+-i-n Diode With Al+ Ion-Implanted Emitters," IEEE Trans. Electron Devices, vol. 65, no. 2, pp. 629–635, Feb. 2018.

[13] K. Schuster and E. Spenke, "The voltage step at the switching of alloyed pin rectifiers," Solid. State. Electron., vol. 8, no. 11, pp. 881–882, Nov. 1965.

[14] L. W. Davies, "The Use of P-L-N Structures in Investigations of Transient Recombination from High Injection Levels in Semiconductors," Proc. IEEE, vol. 51, no. 11, pp. 1637–1642, 1963.

[15] S. Bellone and G. D. Licciardo, "An analog circuit for accurate OCVD measurements," IEEE Trans. Instrum. Meas., vol. 57, no. 6, pp. 1112–1117, 2008.

[16] H. Schlangenotto and W. Gerlach, "On the post-injection voltage decay of p-s-n rectifiers at high injection levels," Solid State Electron., vol. 15, no. 4, pp. 393–402, 1972.

[17] M. A. Green, "Minority carrier lifetimes using compensated differential open circuit voltage decay," Solid. State. Electron., vol. 26, no. 11, pp. 1117–1122, Nov. 1983.

[18] C. Persson, U. Lindefelt, and B. E. Sernelius, "Band gap narrowing in n -type and p -type 3C-, 2H-, 4H-, 6H-SiC, and Si," J. Appl. Phys., vol. 86, no. 8, pp. 4419–4427, Oct. 1999.

[19] T. Kimoto et al., "Nitrogen donors and deep levels in high-quality 4H-SiC epilayers grown by chemical vapor deposition," Appl. Phys. Lett., vol. 67, no. 1995, p. 2833, 1995.

[20] R. Nipoti, A. Parisini, G. Sozzi, M. Puzzanghera, A. Parisini, and A. Carnera, "Structural and functional characterizations of Al+ implanted 4H-SiC layers and al+ implanted 4H-SiC p-n junctions after 1950°C post implantation annealing," ECS J. Solid State Sci. Technol., vol. 5, no. 10, 2016.

[21] R. Nipoti, M. Puzzanghera, and G. Sozzi, "Al+ Ion Implanted 4H-SiC Vertical p+-i-n Diodes: Processing Dependence of Leakage Currents and OCVD Carrier Lifetimes," Mater. Sci. Forum, vol. 897, pp. 439–442, 2017.

[22] P. B. Klein, "Identification and carrier dynamics of the dominant lifetime limiting defect in n-4H-SiC epitaxial layers," Phys. Status Solidi Appl. Mater. Sci., vol. 206, no. 10, pp. 2257–2272, 2009.

[23] G. Sozzi, M. Puzzanghera, R. Menozzi, and R. Nipoti, "The role of defects on forward current in 4h-sic p-i-n diodes," IEEE Trans. Electron Devices, vol. 66, no. 7, pp. 3028–3033, 2019.

[24] S. Lacouture, J. Schrock, E. Hirsch, S. Bayne, H. O'Brien, and A. A. Ogunniyi, "An open circuit voltage decay system for performing injection dependent lifetime spectroscopy," Rev. Sci. Instrum., vol. 88, no. 9, p. 095105, Sep. 2017.

[25] A. Neugroschel, P. J. Chen, S. C. Pao, and F. A. Lindholm, "Diffusion length and lifetime determination in p-n junction solar cells and diodes by forward-biased capacitance measurements," IEEE Trans. Electron Devices, vol. 25, no. 4, pp. 485–490, 1978.